Investigations on Calibration Sources for Soft X-Ray Plasma Spectroscopy and Impurity Monitors

U. Schumacher, K. Asmussen, G. Fußmann,
T. Liebsch, R. Neu

IPP 8/9 December 1995

Beleg

MAX-PLANCK-INSTITUT FÜR PLASMAPHYSIK

85748 GARCHING BEI MÜNCHEN

MAX-PLANCK-INSTITUT FÜR PLASMAPHYSIK

GARCHING BEI MÜNCHEN

Investigations on Calibration Sources for Soft X-Ray Plasma Spectroscopy and Impurity Monitors

U. Schumacher[1], K. Asmussen, G. Fußmann[2],
T. Liebsch[3], R. Neu

IPP 8/9 December 1995

Max-Planck-Institut für Plasmaphysik, EURATOM Association
85748 Garching
[1] Institut für Plasmaforschung, Universität Stuttgart, 70569 Stuttgart
[2] MPI für Plasmaphysik, Bereich Berlin, Mohrenstr. 40/41, 10117 Berlin
[3] Fritz-Haber-Institut der Max-Planck-Gesellschaft, 14195 Berlin

Die nachstehende Arbeit wurde im Rahmen des Vertrages zwischen dem Max-Planck-Institut für Plasmaphysik und der Europäischen Atomgemeinschaft über die Zusammenarbeit auf dem Gebiete der Plasmaphysik durchgeführt.

Investigations on Calibration Sources for Soft X-Ray Plasma Spectroscopy and Impurity Monitors

U. Schumacher[1], K. Asmussen, G. Fußmann[2], T. Liebsch[3], R. Neu

Max-Planck-Institut für Plasmaphysik, EURATOM-Association, 85740 Garching, Germany

[1] Institut für Plasmaforschung, Universität Stuttgart, 70569 Stuttgart, Germany
[2] MPI für Plasmaphysik, Bereich Berlin, 10117 Berlin, Germany
[3] Fritz-Haber-Institut der Max-Planck-Gesellschaft, 14195 Berlin, Germany

Abstract

For absolute soft X-ray line intensity measurements of magnetically confined plasmas large-area X-ray sources for K-, L- and M-transitions of different elements covering a wide photon energy (and wavelength) range are investigated. From the absolute line intensities the quantum efficiency values of several elements are deduced. They represent the basis of simple soft X-ray monitors for impurities in fusion plasmas.

1. Introduction

The fractional abundances and the spatial concentrations of impurities belong to the most important quantities to be determined in magnetically confined fusion plasmas. Light impurities lead to dilution of the fuel, heavier impurities contribute to radiative losses of the core plasma.

Although impurities therefore seem to be undesirable in fusion plasmas, a certain concentration and spatial distribution might play an important role in controlling the energy transport distribution and the radiative energy loss in a fusion reactor.

Absolute impurity concentrations can be deduced from absolute intensity measurements of X-ray lines of the impurity elements in question. Besides the determination of important plasma parameters this is one of the main aims of plasma spectroscopy [1].

For isotropic emission without reabsorption the line intensity I_L is given by the integral of the local line emission coefficient along the line of sight of the spectrometer or monochromator

$$I_L = \frac{1}{4\pi} \int h\nu \cdot A \cdot n_a \cdot dl ,$$

where $h\nu$ is the photon energy, A the transition probability, dl the element along the line of sight and n_a the density of the excited atoms which emit the radiation. For hydrogen-like ions of most of the impurities in a fusion plasma the density n_a of the excited level for the

emission of Lyman lines can be related to the respective impurity concentration C_x by assuming corona population equilibrium. For these assumptions

$$I_L = \frac{1}{4\pi} \int h\nu \cdot n_e^2 \cdot f_x \cdot \langle \sigma v_e \rangle \cdot C_x \cdot A/\Sigma A_a \cdot dl,$$

where n_e is the electron density, f_x the fractional abundance of the hydrogen-like ionisation state, $\langle \sigma\ v_e \rangle$ the electron collisional excitation rate and $\Sigma\ A_a/A$ the branching ratio. After a deconvolution of spatially resolved line intensity measurements (Abel inversion) the impurity concentration C_x can be obtained from the line intensities I_L on the basis of the knowledge of the electron density n_e and the atomic physics parameters.

The sensitivity (or the throughput) of an X-ray monochromator or spectrometer for absolute line intensity measurements depends on a number of properties of the spectrometer components involved as acceptance area, solid angle, reflectivities, transmissions, detector efficiencies, etc. [2]. These properties can only be determined separately. Since the accuracy, which can be achieved for every parameter, is limited, the error for the total sensitivity is too large. Hence it is desirable to have an absolutely calibrated X-ray source. Since the magnetically confined plasmas are extended volume X-ray sources, the calibration device must be a large-area X-ray source of high uniformity and very good reproducibility [3]. Moreover, a very large spectral range should be available for absolute calibration.

2. Characteristic X-ray Line Calibration for Impurity Monitoring

Characteristic X-ray lines are very advantageous for calibrating Lyman line intensities of the plasma impurities. Normally the Lyman lines are well separated in the soft X-ray spectrum. They are emitted from the ionization stage that is near to the plasma center, and - if coronal ionisation equilibrium is fulfilled - the impurity concentration can easily be deduced from their intensity. There exist X-ray sources using K-, L- and M-transitions of various elements, that can easily be applied for calibrating the Lyman lines in question:

Cl Lyman α (Cl XVII 1s - 2p at λ = 0,4187 nm) can be calibrated with Ag $L\alpha_{1,2}$ (λ = 0.4155 nm), for Ne Lyman α (Ne X 1s - 2p at 1.2148 nm) Zn $L\alpha_{1,2}$ (λ = 1.2282 nm) or Na Kα (λ = 1.1909 nm) would be appropriate X-ray calibration lines, O Lyman α (O VIII 1s -2p at λ = 1.8969 nm) is in the wavelength vicinity of F Kα (λ = 1.8307 nm), and for the calibration of C Lyman α (C VI 1s - 2p at λ = 3.3736 nm) the line N Kα (λ = 3.1603 nm) might be used. In Table 1 the Lyman α and the Helium-like resonance lines w of some of the elements typical for present-day magnetically confined plasmas are listed together with the corresponding X-ray calibration lines.

Since the magnetic confinement fusion experiments presently work with wall materials of atomic numbers as low as possible (applying carbonization and boronization of the vessel walls or even Be limiters), the respective photon energies approach very low values. This, however, leads to severe difficulties for the calibration sources and for the monochromator systems mainly due to the increasing absorption coefficients towards longer wavelength [4]. Recent developments, however, tend to apply medium-Z impurities (like Ne) for radiation

cooling of the boundary layer or to investigate even high-Z materials (like W) as possible divertor plates.

To explore the large-area X-ray sources for calibration devices an investigation of absolute line intensities of K-, L- and M-transitions of different elements covering a wide range of photon energies (and wavelengths) was performed.

3. X-ray Impurity Monitoring

The Lyman α-lines and the corresponding characteristic X-ray lines that usually occur in magnetically confined plasmas cover a wide range of wavelengths λ and photon energies ε. This wavelengths range over two orders of magnitude is illustrated in Fig. 1. The abscissa gives the wavelength λ (below) and the photon energy ε (on top) with the location of some of the characteristic X-ray calibration lines. With the lattice constant 2d of crystals as ordinate it is obvious, that a very limited number of different crystals is sufficient for first order Bragg reflection in the Bragg angle range from about 10° to 90°.

This first order Bragg reflection is the basis for simple X-ray impurity monitors [4, 5]. In contrast to the broad-band impurity survey monochromators and high-resolution X-ray spectrometers which due to their high flexibility offer different investigations of the impurity behaviour, X-ray impurity monitors have to be simple, consisting only of a collimator, a flat crystal at fixed angular position and a proportional counter.

These devices are based on the intensity measurement of the Lyman-α (1s - 2p) transitions of the most important low-Z impurities. Fig. 2 gives a scheme for a monitor for carbon, oxygen and neon. Their Lyman-α-transitions (C VI 1s - 2p at λ = 3.3736 nm, O VIII 1s - 2p at λ = 1.8967 nm and Ne X 1s - 2p at λ = 1.2134 nm) can be monitored by proportional counters measuring the X-ray beams collimated by multi-grid collimators and reflected in first order off KAP (001) crystals and a PX 1 multilayer, respectively. A detailed description and the results of the carbon and oxygen monitor at the tokamak ASDEX-Upgrade are given in [11].

These monitors as impurity survey instruments need to be calibrated for absolute impurity concentration measurements [4]. From the measured absolute line intensity $I = \int \varepsilon dl$ an emission coefficient $\bar{\varepsilon}$ averaged over the line of sight through the emission layer of the line in question is inferred with the known electron density and temperature profile. As an extension of corona ionisation equilibrium the impurity transport is to be taken into account if an accuracy of better than about 50 % is aimed at. Neglecting the contribution of charge exchange processes the averaged emission coefficient depends only on the electron density n_e, the ground state density n_1 of the hydrogen-like ion in the emission layer and on the electron collisonal excitation rate C_{12} into the second main quantum number.

4. The Large-area X-ray Calibration Source

The calibration sources consist of a large-area solid metal plate of an area of 10 x 30 cm^2 and 7 x 10 cm^2, respectively, as anode and - parallel to the anode surface - of a system of stretched thin gold-covered tungsten wires 100 μm in diameter as cathode. The wires have

a distance of 4 mm from each other. They are heated to emit electrons which are accelerated towards the anode. The anode plate is - insulated from the vacuum vessel and cathode structure - at high voltage. A scheme of the source is given in Fig. 3. The anode plates can easily be exchanged in order to obtain different K-, L- and M-characteristic X-ray lines. They are mounted on and in thermal contact to a block which is cooled by silicone oil. The X-rays are observed through the cathode mesh.

5. Results

For a pressure in the vacuum vessel which is less than about 10^{-3} Pa one obtains stable and reproducible emission characteristics with excellent homogeneity over the anode area. The X-ray emission is proportional to the electron current density within a relatively wide range.

For an anode voltage of 20 kV (electron energy of 20 keV) and an electron current density of $j = 0.032$ A m^{-2} the measured absolute line intensities of K-, L- and M-transitions of different elements are plotted in Fig. 4 versus the photon energy E and wavelength λ, respectively. The absolute calibration of this large-area X-ray source was obtained from the count rate of a Si (Li) detector for known values of solid angle, aperture area and spectral efficiency [6]. For Mn Kα (solid dot in Fig. 4), moreover, the calibration was made utilizing a calibrated ^{55}Fe source. The absolute calibration for photon energies below about 1 keV is hampered - as mentioned before and as expressed by Campbell [10]- by absorption processes in foils and detector.

For the K-transitions the measurements (open circles) are compared to the calculated values obtained from the formula of M. Green [7] for the number of characteristic X-rays per electron of energy E_0 [in keV], which hits the target. This formula gives a line intensity (radiance) of

$$I_{line}[Wm^{-2}sr^{-1}] = (10^3/4\pi)\cdot K_0\cdot (E_0-E_x)^{1.63}\cdot j\cdot E_x\cdot f,$$

where K_0 is the quantum efficiency as given by Green and Cosslett [9], E_x is the minimum exciting voltage for these characteristic X-rays in keV, j is the electron current density in A m^{-2} and f is the correction factor due to absorption by the target itself [8]. As to be seen from Fig. 4 there is good agreement between the experimental and calculated intensity values (except for titanium as anode material). It is important to note, that there is no fit parameter to be applied. The only quantity to apply is the value of K_0 by Green. This fact not only is valid for pure chemical elements (like the metals) but also for crystals (like InSb) or alloys (like Brass or Inconel), for which the characteristic line intensity is proportional to the chemical concentration. The intensity sum, plotted at the average energy fits into the curve.

Furthermore there is excellent agreement found between the measurements of the intensity as a function of the acceleration voltage (electron energy) E_0 and the corresponding intensity values calculated according to Green and Cosslett [9]. Fig. 5 gives an example of the Fe Kα intensity ($\hbar\omega_{K\alpha}$ = 6.399 keV) emitted from an iron anode as a function of the anode voltage. The measurements (open circles) are in remarkable quantitative agreement with the calculated intensity values (solid line) and reflect the $(E_0 - E_x)^{1.63}$ dependence of the intensities.

On the basis of the absolute line intensity measurements of the different K-, L-, and M-transitions an extension of the quantum efficiency values K_o beyond those given by Green is possible. These quantum efficiencies K_o are plotted in Fig. 6 versus the atomic number Z. The full circles belong to the Kα-lines; they follow the full line given by Green and Cosslett [9], while the dashed line connects the quantum efficiencies for Lα+β-lines (open circles). The quantum efficiencies of some Lβ-, Lγ-, and M-transitions are added, too.

Acknowledgements

The authors are grateful to Drs. G. Janeschitz, H.W. Morsi and H. Röhr for many fruitful discussions and to J. Fink, M. Hien and G. Schmitt for continuous support.

References

[1] S. von Goeler, M. Bitter, S. Cohen, D. Eames, K.W. Hill, D. Hills, R. Hulse, G. Lenner, D. Manos, P. Roney, N. Sauthoff, S. Sesnic, W. Stodiek, F. Tenney, J. Timberlake, Proc. Course on Diagnostics for Fusion Reactor Conditions, ed. P.E. Stott et al. (CEC Brussels 1983) Vol.I, P.109

[2] R. Barnsley, U. Schumacher, E. Källne, H.W. Morsi, and G. Rupprecht, Rev. Sci. Instrum. 62, 889 (1991)

[3] H. Morsi, H. Röhr, and U. Schumacher, Z. Naturf. 42a, 1051 (1987)

[4] U. Schumacher, R. Barnsley, G. Fussmann, K. Asmussen, C.C. Chu, G. Janeschitz, AIP Conf. Proc. 257, Atomic Processes in Plasmas, p.131 (1992)

[5] G. Janeschitz, private communication

[6] P. Müller, F. Riehle, E. Tegeler and B. Wende, Nucl. Instrum. Meth. A 246, 569 (1986)

[7] M. Green, X-ray Optics and X-ray Microanalysis, Academic Press, N.Y., London 1963, p.185; M. Green, Proc. Phys. Soc. 83, 435 (1964).

[8] T. Rao-Sahib, D. Wittry, J. Appl. Phys. 45, 5060 (1974).

[9] M. Green, V.E. Cosslett, Brit. J. Appl. Phys. 1, 425 (1968); M. Green, V.E. Cosslett, Proc. Phys. Soc. 78, 1206 (1961).

[10] A.J. Campbell, Proc. Roy. Soc. A274, 319(1963).

[11] R. Neu, K. Asmussen, G. Fußmann, P. Geltenbort, G. Janeschitz, K. Krieger, K. Schönmann, G. Schramm, U. Schumacher, submitted to Rev. Sci. Instrum.

Figure captions

Fig. 1: Wavelength and Bragg angle positioning for first-order flat crystal reflection of Lyman α - and characteristic X-ray lines.

Fig. 2: Scheme of an X-ray monitor for C, O, and Ne.

Fig. 3: Scheme of the large-area X-ray calibration source (cross-section).

Fig. 4: K-, L- and M-transition absolute line intensities of different elements compared to the calculated values. For the alloys brass and Inconel the intensity sum is plotted at the average energy E. The full dot indicates the additional calibration with Mn Kα by the calibrated ^{55}Fe source. Moreover, averaged values for the alloys inconel and brass are included.

Fig. 5: Fe Kα intensities measured as function of the electron energy E_o for a current density of j = 0,143 Am^{-2} (dots) compared to the calculated intensities using a quantum efficiency of $2{,}6 \cdot 10^{-5}$ given by Green and Cosslett [9] (solid line).

Fig. 6: Quantum efficiency values K_o versus atomic number Z, added to and compared to values of Green and Cosslett [9] (solid line).

Table 1

Element	Lyman α line $1s\ ^2S - 2p\ ^2P^o$	Calibration line		Helium-like resonance line W $1s^2\ ^1S - 1s2p\ ^1P^o$	Calibration line	
	Wavelength [nm]	type	Wavelength [nm]	Wavelength [nm]	type	Wavelength [nm]
Be	7.5928	B Kα	6.7	10.02552	Be Kα	11.3937
B	4.8588	C Kα	4.4000	6.03144	B Kα	6.7
C	3.3736	N Kα Ca $L\alpha_{1,2}$	3.1603 3.6393	4.0268	C Kα Ca $L\alpha_{1/2}$	4.4 3.6393
O	1.8969	F Kα Mn $L\alpha_{1,2}$	1.8307 1.9489	2.1602	O Kα Cr $L\alpha_{1/2}$	2.3707 2.1713
Ne	1.2134	Na Kα Zn $L\alpha_{1,2}$	1.1909 1.2282	1.3447	Cu $L\alpha_{1/2}$	1.3357
Cl	0.4187	Ag $L\alpha_{1,2}$	0.4155	0.44442	Cl Kα Pd Lα1,2	0.4729 0.4372
Ar	0.3733	K Kα	0.3744	0.39488	K Kα Cd $L\alpha_{1/2}$	0.3744 0.396
Cr	0.2092	Mn Kα	0.2103	0.2192	Mn Kα Sm $L\alpha_{1,2}$	0.2103 0.2205
Fe	0.1780	Co Kα	0.1791	0.18503	Fe Kα co Kα Ho $L\alpha_{1/2}$	0.1937 0.1791 0.185
Ni	0.1532	Cu Kα	0.1542	0.1588	Cu Kα Hf $L\alpha_{1,2}$	0.1542 0.1575
Cu	0.1427	Zn Kα	0.1437	0.1478	Zn Kα W $L\alpha_{1,2}$	0.1437 0.1476

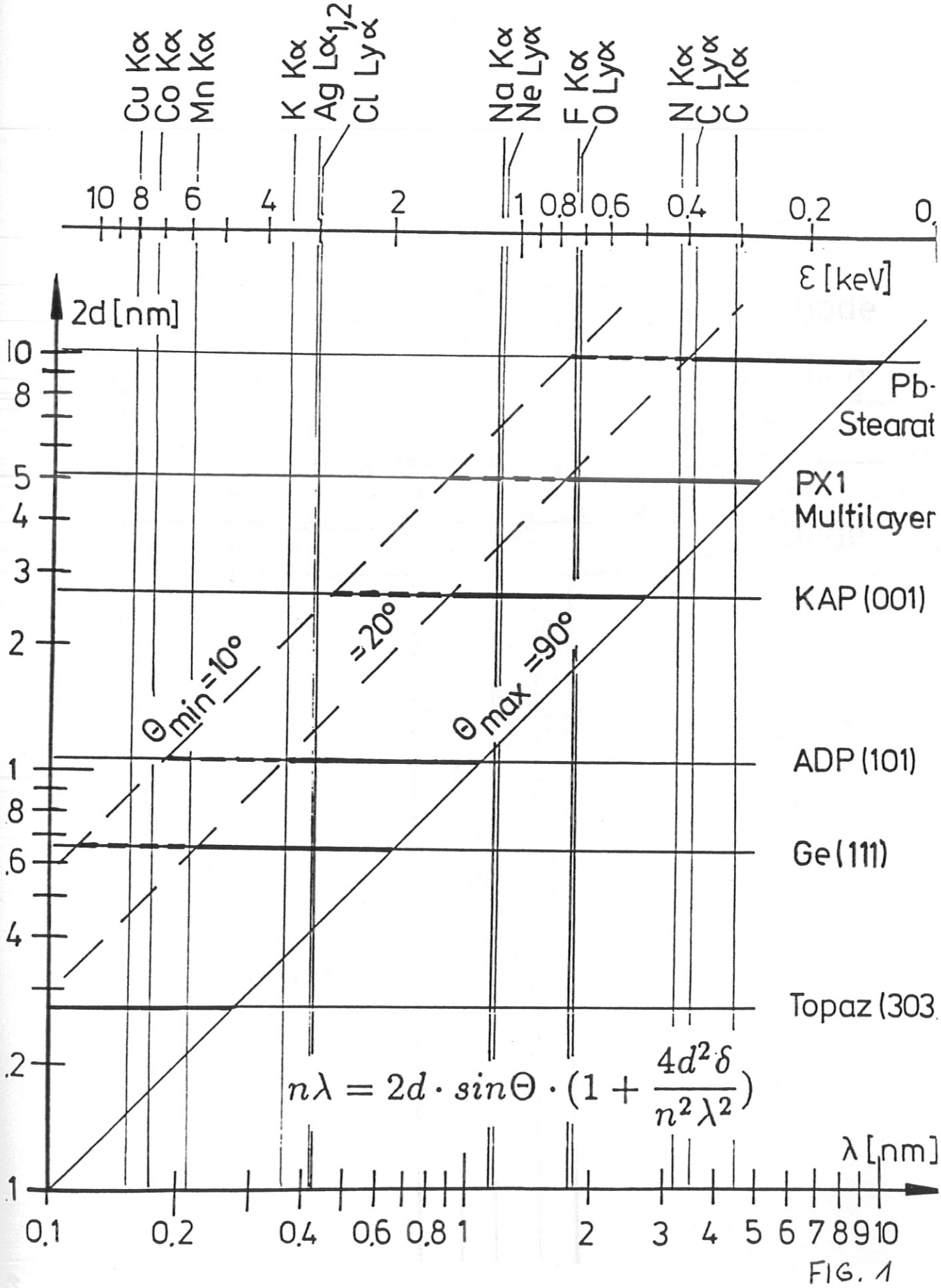
Cu Kα
Co Kα
Mn Kα
K Kα
Ag Lα1,2
Cl Lyα
Na Kα
Ne Lyα
F Kα
O Lyα
N Kα
C Lyα
C Kα
10 8 6 4 2 1 0.8 0.6 0.4 0.2 0
ε [keV]
2d [nm]
10
8
5
4
3
2
1
.8
.6
.4
.2
1
Pb-Stearat
PX1 Multilayer
KAP (001)
ADP (101)
Ge (111)
Topaz (303
Θmin=10°
=20°
Θmax=90°
$n\lambda = 2d \cdot \sin\Theta \cdot (1 + \frac{4d^2\delta}{n^2\lambda^2})$
λ [nm]
0.1 0.2 0.4 0.6 0.8 1 2 3 4 5 6 7 8 9 10

FIG. 1

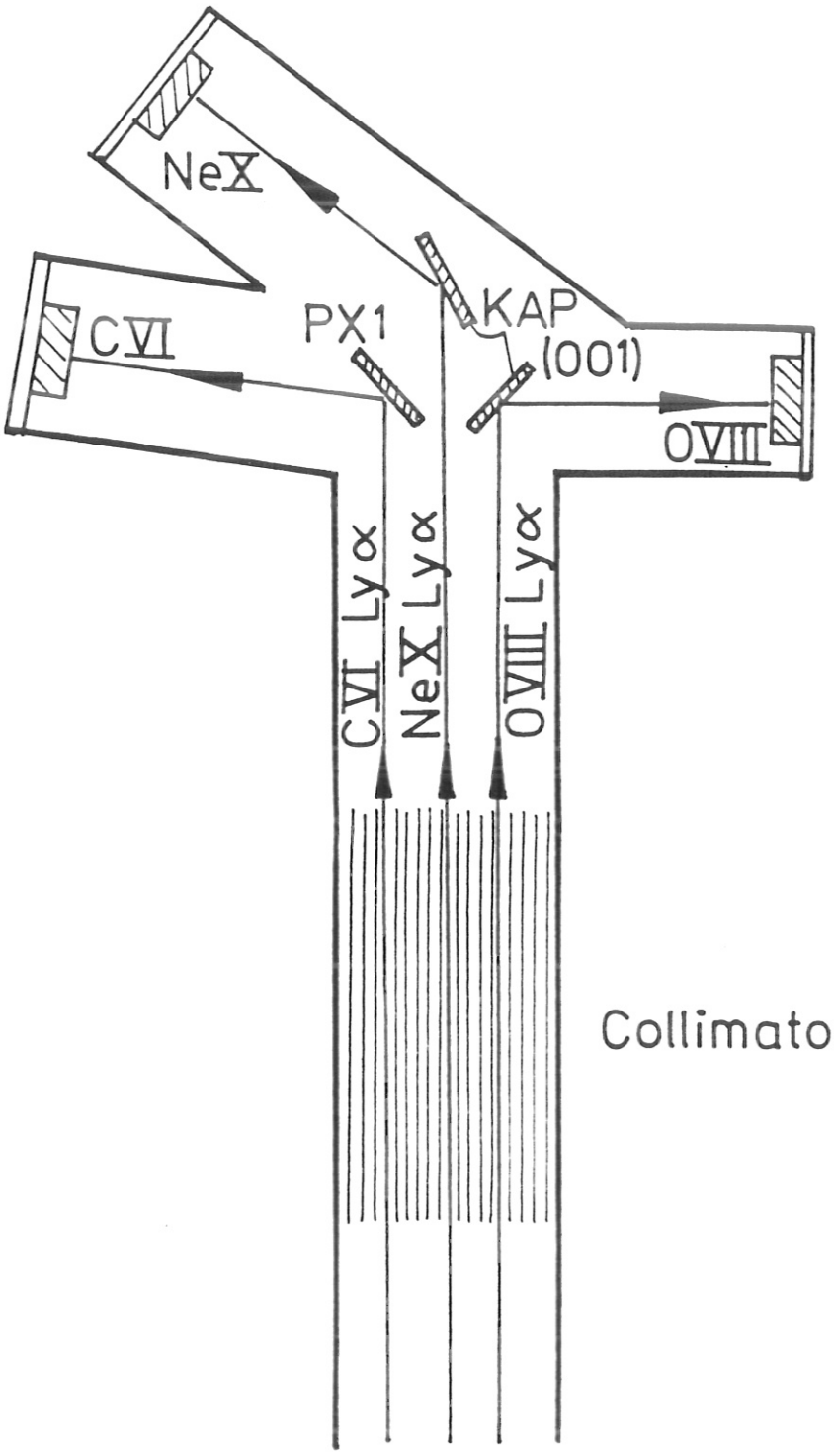
NeX
CVI
PX1
KAP
(001)
OVIII
CVI Lyα
NeX Lyα
OVIII Lyα
Collimator

FIG. 2

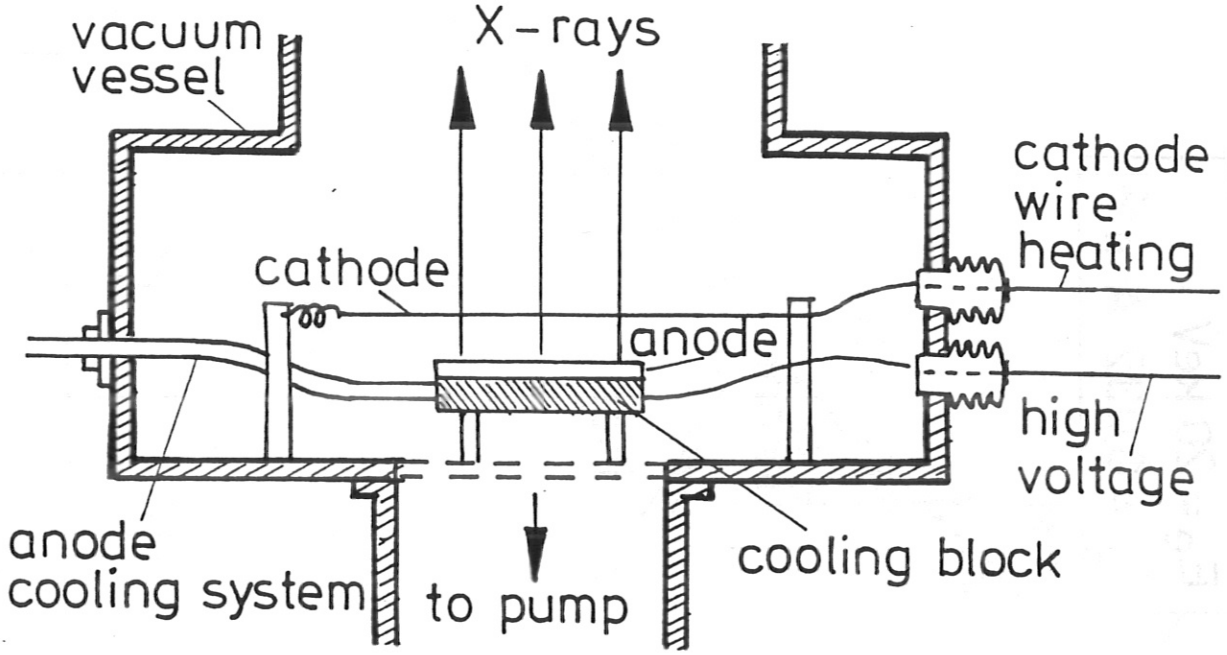
vacuum
vessel
X-rays
cathode
wire
heating
cathode
anode
high
voltage
anode
cooling system
to pump
cooling block

FIG. 3

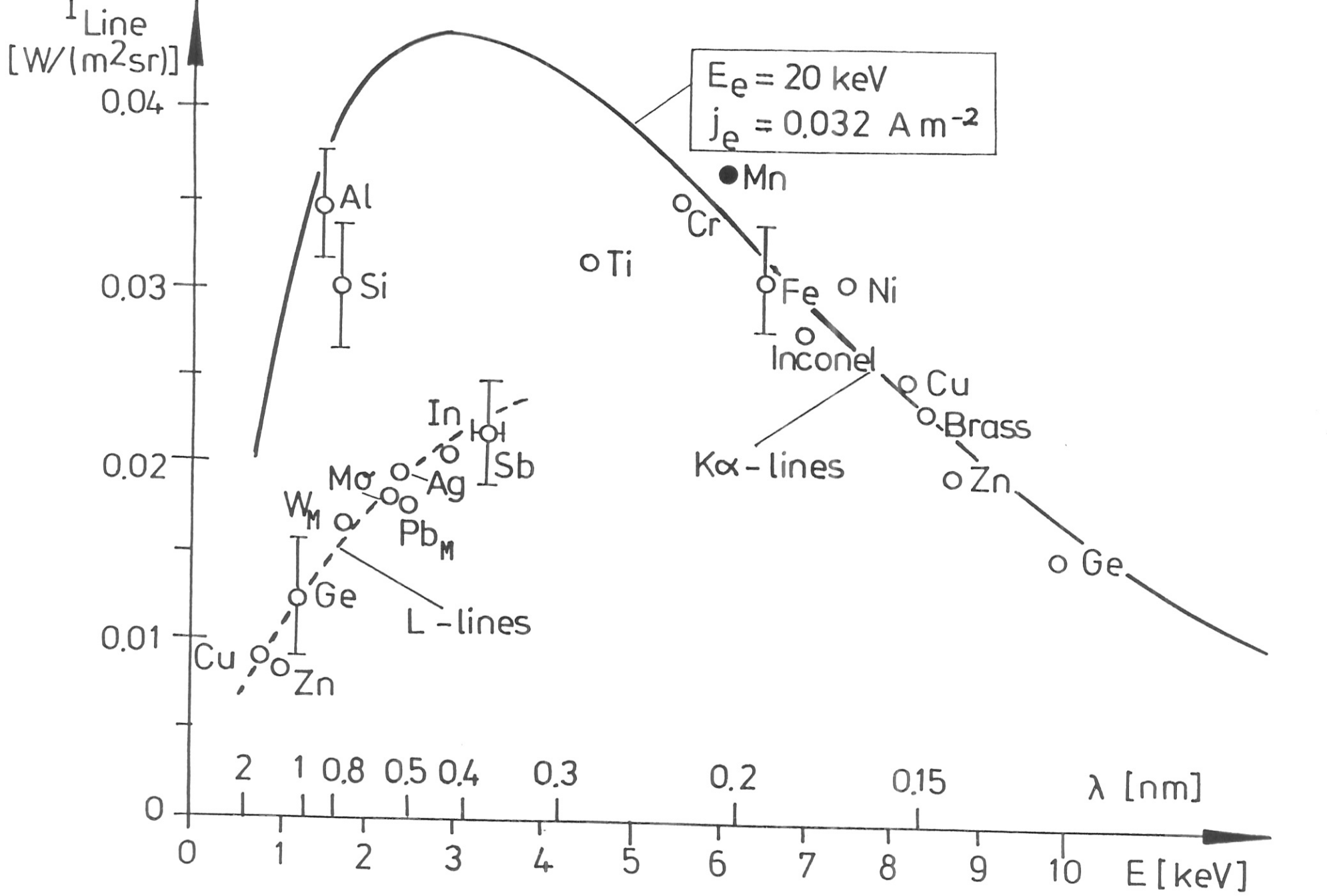
I Line [W/(m2sr)]
0.04
0.03
0.02
0.01
0
Ee = 20 keV
je = 0.032 A m-2
Mn
Al
Si
Ti
Cr
Fe
Ni
Inconel
Cu
Brass
Zn
Ge
Kα - lines
In
Sb
Mσ
Ag
WM α
PbM
Ge
L - lines
Cu
Zn
2 1 0.8 0.5 0.4 0.3 0.2 0.15 λ [nm]
0 1 2 3 4 5 6 7 8 9 10 E [keV]

FIG. 4

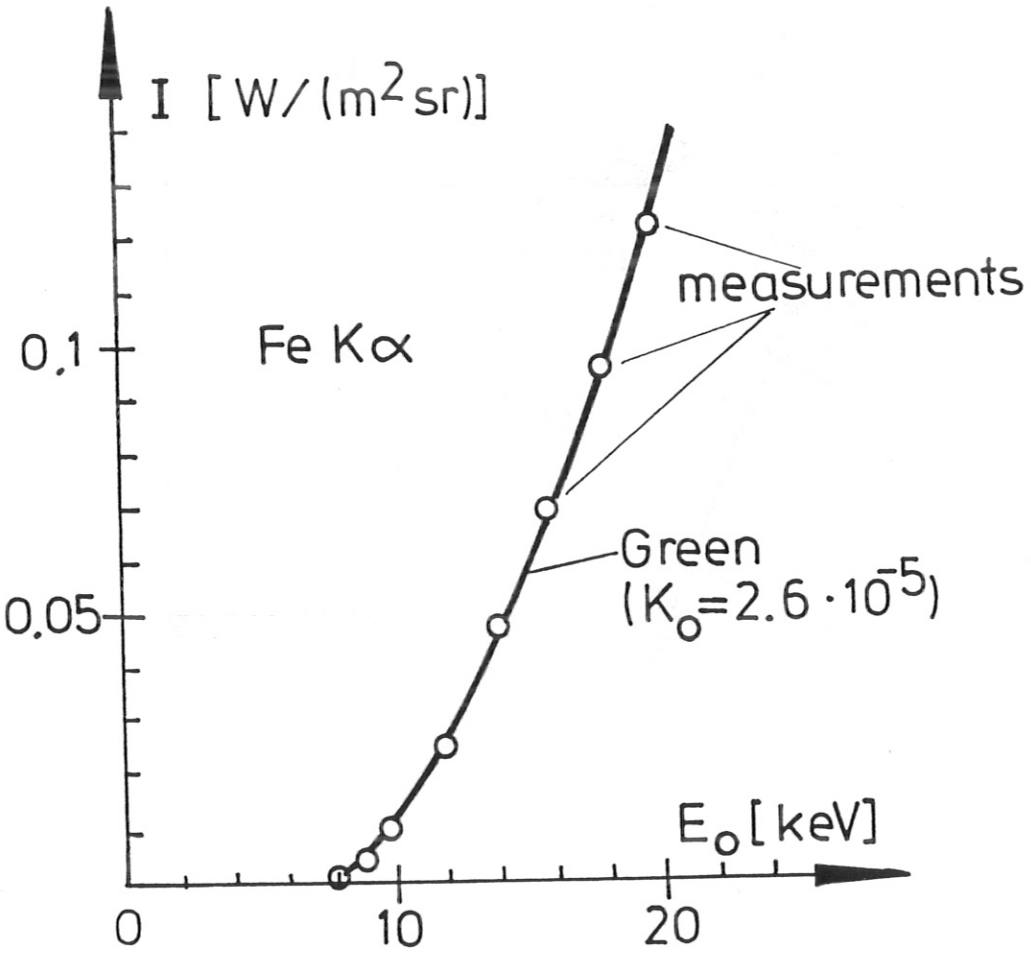

FIG. 5

FIG. 6

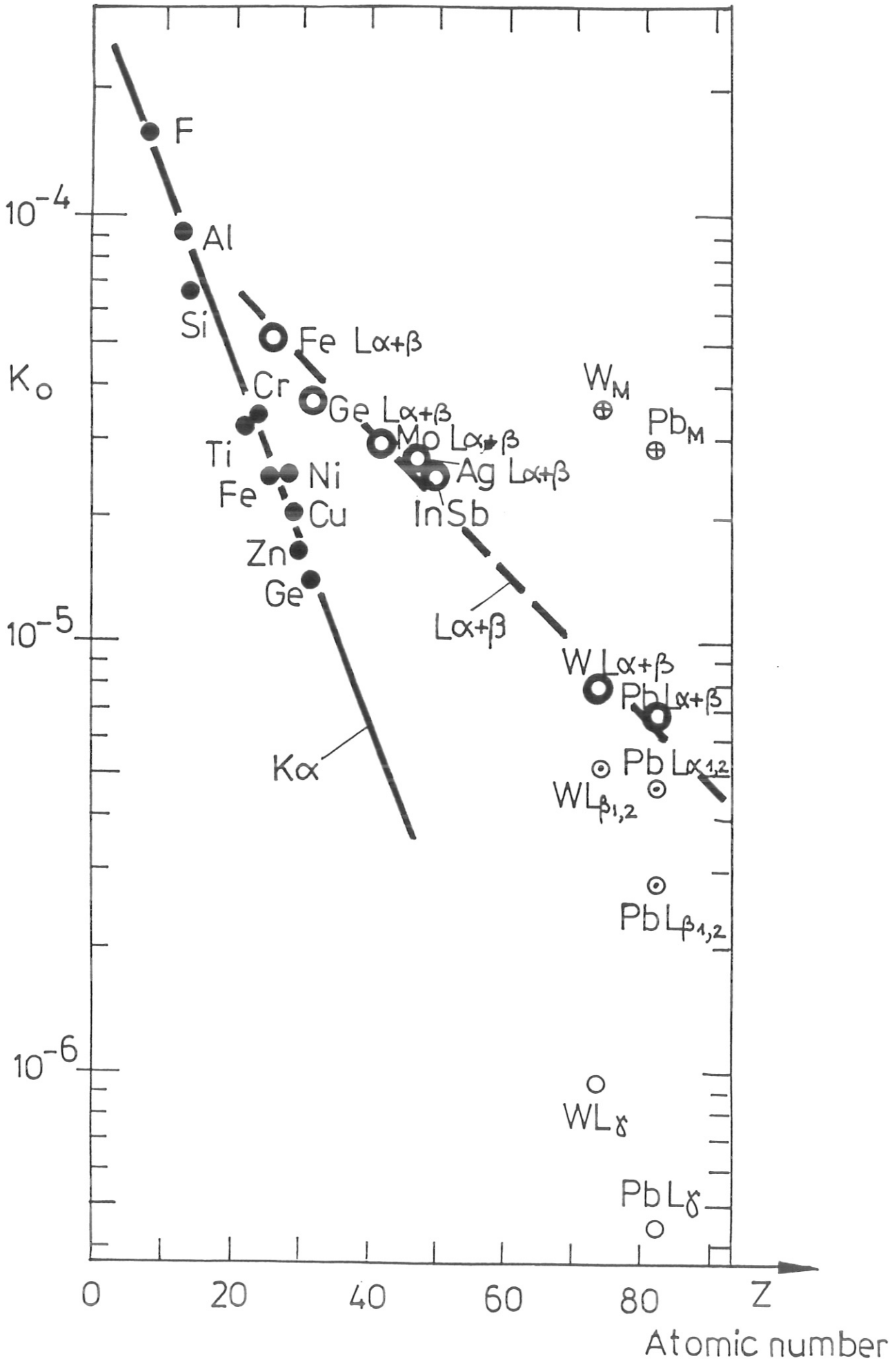
F
Al
Si
Fe Lα+β
Cr
Ge Lα+β
Mo Lα+β
Ti
Ni
Fe
Ag Lα+β
Cu
InSb
Zn
Ge
Lα+β
Kα
W Lα+β
Pb Lα+β
Pb Lα1,2
WLβ1,2
PbLβ1,2
WLγ
PbLγ
WM
PbM
10^{-4}
10^{-5}
10^{-6}
K_o
0
20
40
60
80
Z
Atomic number